ELSEVIER

Chemical Engineering Journal 138 (2008) 136–147

Chemical Engineering Journal

www.elsevier.com/locate/cej

Characterization of a flat plate photobioreactor for the production of microalgae

E. Sierra, F.G. Acién, J.M. Fernández, J.L. García, C. González, E. Molina *

Department of Chemical Engineering, University of Almería, E-04071 Almería, Spain

Received 2 March 2007; received in revised form 5 June 2007; accepted 6 June 2007

Abstract

This paper presents the characterization of a flat panel photobioreactor (0.07 m wide, 1.5 m height and 2.5 m length) for the production of microalgae. Several factors are considered. The orientation was studied first resulting east/west the most favourable because the total solar radiation intercepted was maximum, increasing 5% with regard to horizontal placement, and the exposure resulted to be the most homogeneous over the year. Then, gas holdup, mass transfer, mixing and heat transfer were studied as a function of the aeration rate. This is a key operating variable because it determines the power supply, which governs the fluid-dynamics of the system and subsequently influences other transport phenomena. The gas holdup and mass transfer coefficient found were consistent with referenced values for bubble columns observed in tubular photobioreactor. A power supply of 53 W/m^3 promoted a mass transfer rate high enough to avoid the excessive accumulation of dissolved oxygen in this flat panel photobioreactor. This is similar to the 40 W/m^3 necessary in bubble columns and much lower than the 2000–3000 W/m^3 required in tubular photobioreactors. However, this power supply is in the order of magnitude of 100 W/m^3, which has been reported to damage some microalgal cells, whereas no damage has been referenced in tubular photobioreactors. Even at low power supplies the mixing time was shorter than 200 s, longer than the 60 s measured for bubble columns, but quite faster than the typical values found for tubular photobioreactors (1–10 h). With regard to heat transfer, global coefficients were determined for the internal heat exchanger and for the external surface of the photobioreactor. The observed behaviour was similar to that referenced for bubble columns, although the values of heat transfer coefficients measured were lower than in bubble columns. The heat transfer coefficient of the internal heat exchanger (over 500 W/m^2 K) was much higher than the coefficient of the external surface of the reactor (30 W/m^2 K). Internal heat exchangers are therefore useful to control the temperature of the culture in this type of photobioreactor. The major disadvantage of this reactor is the potential high stress damage associated with aeration. The main advantages are the low power consumption (53 W/m^3) and the high mass transfer capacity (0.007 1/s). The characterization carried out allows improving the design and establishing the proper operating conditions for the production of microalgae using this type of photobioreactor.

Keywords: Mass transfer; Mixing; Heat transfer; Microalgae; Photobioreactor

1. Introduction

Microalgae have been cultured by mankind for centuries, mainly as food. In the past few decades, most of the research in this field has aimed to the development of open outdoor mass cultures, resulting in the large-scale production facilities currently in operation throughout the world [1]. Such systems are inexpensive but have important drawbacks. Open systems cannot ensure a contamination-free monoalgal operation. The culture conditions are poorly controlled and only a few resistant microalgal strains can grow under the extreme conditions (high pH, salinity or temperature) that normally take place in open systems. The fact is that most microalgal strains can only be cultured under controlled conditions and protected from the environment. This is only possible with fully closed photobioreactors [2]. Closed photobioreactors are suitable for the production of strains rich in high value products, and also allow taking advantage of the metabolic flexibility of microalgae: the generation rate of desired product can be enhanced by setting the proper culture conditions. The design of closed photobioreactors must be carefully optimized for each individual algal species, according to its unique physiological and growth characteristics [3]. Two dominant environmental factors require substantial attention: sunlight

* Corresponding author at: Department of Chemical Engineering, University of Almería, Cañada San Urbano S/N, 04071 Almería, Spain.
Tel.: +34 950 015032; fax: +34 950 015484.
E-mail address: emolina@ual.es (E. Molina).

1385-8947/$ – see front matter © 2007 Elsevier B.V. All rights reserved.
doi:10.1016/j.cej.2007.06.004

Nomenclature

A	external area of the heat exchanger (m^2)
C	concentration of dissolved oxygen (mol/m^3)
Cp	heat capacity (kJ/kg K)
d	light-path of the reactor (m)
Dc	diameter of the system (m)
Dz	dispersion coefficient (m^2/s)
E	function of residence time at the outlet
Fr	Fraudre number
g	gravitational acceleration (m/s^2)
G	hourly global radiation on a horizontal surface (kJ/m^2 s)
G_r	reflected hourly radiation on a tilted surface (kJ/m^2 s)
G_{rb}	direct hourly radiation on a tilted surface (kJ/m^2 s)
G_{rd}	diffuse hourly radiation on a tilted surface (kJ/m^2 s)
h	individual heat transfer coefficient by convection (W/m^2 K)
hs	solar time (h)
H	daily global radiation on a horizontal surface (kJ/m^2 s)
H_b	daily global direct radiation on a horizontal surface (kJ/m^2 s)
H_d	daily global disperse radiation on a horizontal surface (kJ/m^2 s)
H_o	extraterrestrial daily global radiation (kJ/m^2 s)
I_{sc}	solar irradiance constant (kJ/m^2 s)
k_L	thermal conductivity of the liquid (kJ/h m K)
Kh	transparency index of the atmosphere
K_La_L	overall volumetric mass transfer coefficient (1/s)
L	total length of the reactor (m)
m_{OH}	total amount of alkali injected (mol)
m_{water}	mass flow of hot water through the heat exchanger (kg/s)
N	day of the year
Nd	dimensionless dispersion number
P_G	power supply by aeration (J/s)
Pr	dimensionless Prandtl number
Q_L	liquid flow rate (m^3/s)
R_b	ratio of direct to total radiation on a tilted surface
R_d	ratio of diffuse to total radiation on a tilted surface
Re	dimensionless Reynolds number
S	cross-section of the reactor (m^2)
t	time (s)
t_m	mixing time (s)
t_r	residence time (s)
T	temperature (K)
U	overall heat transfer coefficient (W/m^2 K)
U_G	superficial gas velocity in the aerated zone (m/s)
V	total volume of the reactor (m^3)
V_L	volume of liquid (m^3)

Greek letters

β	hourly radiation on an tilted surface (degrees)
δ	declination (degrees)
ε	overall gas holdup
ϕ	latitude (degrees)
γ	solar angle with respect to the south (degrees)
μ_L	liquid viscosity (kg/m^2 s)
θ	solar angle of a surface (degrees)
θ_t	dimensionless time
θ_z	Azimuthal angle (degrees)
ρ_L	density of the liquid (kg/m^3)
σ^2	variance
ω	solar angle (degrees)
ω_s	sunrise solar angle (degrees)

and temperature [4,5]. Also other design parameters such as light regime, heat and mass transfer must be fine tuned for proper operation [6,7].

For this reason, a variety of closed photobioreactors have been proposed to suit the particular characteristics of different microalgal strains. The designs range from horizontal tubular systems [8,9], to helical tubular reactors [10], cascade reactors [11], alveolar flat panels [12], vertical flat panels [13] or bubble columns [42]. The most scaleable designs correspond to horizontal or helical tubular systems, as well as combinations of vertical flat panels and bubble columns, and so these types of photobioreactors have attracted most interest. An integrated characterization of solar radiation, fluid-dynamic and mass transfer of both tubular and bubble column photobioreactors are already available [14,15,42], but flat panel photobioreactors have been disregarded this far.

Flat panel photobioreactors feature important advantages for mass production of photoautotrophic microorganisms and may become a standard reactor type for the mass production of several algal species. The construction of flat plate reactors dates back to the early 1950s [16]. Samon and Leduy [13] used vertically translucent flat plates, illuminated on both sides and stirred by aeration. Tredici and Materassi developed this idea [12,17] proposing a rigid alveolar panel. Pulz et al. [18] used flat panels with inner walls arranged to promote an ordered horizontal culture flow that was forced by a mechanical pump. The most innovative aspect of the Pulz reactor was that parallel plates were packed together; close enough to attain 6 m^3 of culture volume on 100 m^2 of ground area, with a total illuminated culture surface of ca. 500 m^2. The research of Hu and Richmond [19–21] resulted in a type of flat plate reactor made of glass sheets, glued together with silicon rubber to make flat vessels. This simple methodology for the construction of glass reactors provided the opportunity to easily build reactors with any desired light-path. Recently, a new design of vertical flat panel photobioreactor consisting of a plastic bag located between two iron frames has been proposed [22]; this brings a substantial cost reduction to this type of reactors. In the present paper a flat panel photobioreactors is characterized. The factors considered are the collection

of solar radiation, the power supply necessary to remove oxygen and to avoid nutrient gradients, and the heat transfer capacity for temperature control. The measured behaviour is then compared with other photobioreactors previously analyzed in order to determine the suitability of this type of photobioreactors for the production of microalgae.

2. Materials and methods

2.1. Flat panel photobioreactor

The flat panel photobioreactor featured in Fig. 1 was used. The device consisted of a u-shaped *disposable* plastic bag located between two iron frames 0.070 m apart. Frame and plastic bag are 1.5 m high and 2.5 m long, with a volume of 250 L. The plastic bag is made of free-dispersant 0.75 μm polyethylene, with a transparency index of 0.95 in the photosynthetically active spectrum. The bag can be easily replaced when convenient, excessive fouling or contamination being the most common factors requiring a replacement. A gas sparger (20 mm PVC tube with 1 mm holes every 3 cm) was placed from side to side at the bottom of the plastic bag for aeration, and a heat exchanger consisting of four 2.00 m long, 0.025 m diameter stainless steel tubes was located 0.50 m above the gas sparger inside the bag for temperature control. The air flow rate entering the photobioreactor was regulated using suitable valves and flowmeters (Omega Engineering Inc.). Temperature was controlled passing cool water through the heat exchanger. Dissolved oxygen, pH and temperature probes were located in the upper part of the photobioreactor. Additional temperature probes were installed at the inlet and outlet of the heat exchanger. Environment temperature was also recorded. The data from all the probes was captured by a data acquisition board (DaqFactory, CA, USA) connected to a PC computer for on-line registration and control. A ball valve installed at the bottom allowed wash-out of the reactor. Another ball valve located 1.24 m high, the reactor working level, was used for harvesting during continuous operation.

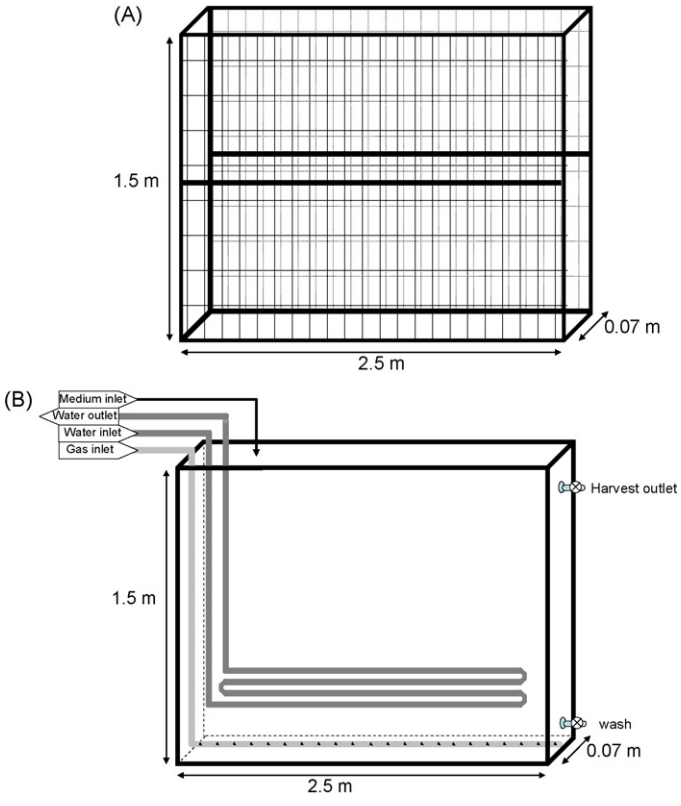

Fig. 1. Schematic drawing of the flat panel photobioreactor used. (A) Frame; (B) schematic drawing of aeration system, heat exchanger, and medium inlet and harvesting valve for the continuous operation of the photobioreactor.

2.2. Fluid-dynamic and mixing characterization

The influence of the air flow rate on the gas holdup and volumetric mass transfer coefficient of the reactor were studied. The overall gas holdup, ε, was determined by the volume expansion method [23]. The overall volumetric mass transfer coefficient, $K_L a_L$, was measured using the dynamic gassing-out method [23]. For $K_L a_L$ measurements, dissolved oxygen was first removed from the reactor by sparging with nitrogen until the dissolved oxygen concentration approached zero. Time was given to allow the N_2 bubbles to disengage and then air was sparged at the required rate. The dissolved oxygen concentration (C) versus time (t) was recorded until close to saturation. For the procedure described, the following well-known equation holds,

$$\frac{dC_L}{dt} = K_L a_L (C^* - C_L) \quad (1)$$

Integration for $C_L = C_0$ at $t = 0$, led to Eq. (2).

$$\ln\left(\frac{C^* - C_L}{C^* - C_0}\right) = -K_L a_L \cdot t \quad (2)$$

A plot of the left hand side of this equation against time was used to obtain $-K_L a_L$ as the slope.

The power input per volume unit due to aeration, P_G/V_L, was calculated as a function of the density of the liquid, ρ_L, the gravitational acceleration, g, and the superficial gas velocity in the aerated zone, U_G.

$$\frac{P_G}{V_L} = \rho_L g U_G \quad (3)$$

Mixing was determined by the pulse–response method, which requires a continuous flow of liquid through the reactor. For this, a pulse of alkaline solution, used as tracer, was injected at the inlet of the reactor, and the tracer concentration was measured at the outlet. These experiments were done using distilled water and air free of CO_2 to avoid influence of bicarbonates buffer. The hydroxyl concentration [OH^-] was determined from pH measurements at the outlet. The residence time function at the outlet, E, and the dimensionless time, θ_t, were then calculated as,

$$E = \frac{[OH^-]}{m_{OH}/V} \quad (4)$$

$$\theta_t = \frac{t}{t_r} \quad (5)$$

where t is the time, m_{OH} the mass of alkali injected and V is the working volume of the reactor. The residence time, t_r, is determined from experimental data as,

$$t_r = \frac{\int_0^\infty t[OH^-]\,dt}{\int_0^\infty [OH^-]\,dt} \quad (6)$$

The consistency of the data was always tested [24] and then for each experiment the variance inside the reactor, σ^2, which represents the mixing degree, was calculated as,

$$\sigma^2 = \int \theta_t^2 E\,d\theta_t - 1 \quad (7)$$

Variance can range from 0, indicating an ideal plug-flow, to 1 obtained for a perfect mixed-tank. This allows identifying the overall behaviour of the system. For real systems, variance values higher than 0.2 are considered to correspond to mixed-tank reactors, while below this value a plug-flow behaviour is accepted. Experiments were performed for different aeration rates keeping a constant liquid flow of 28 L/min. The dispersion coefficient, Dz, which quantifies the mixing as a diffusion-like process and therefore the possible extension of gradients at molecular scale, was calculated from the variance value using the dispersion model [24], and by iterative calculation:

$$\sigma^2 = 2Nd - 2Nd^2\left(1 - \exp\left(\frac{-1}{Nd}\right)\right) \quad (8)$$

$$Dz = \frac{Q_L}{S} \cdot L \cdot Nd \quad (9)$$

where Nd is the dimensionless dispersion number, Q_L the liquid flow rate through the reactor, S the cross-sectional area of the reactor in the direction of the liquid flow (0.07 m × 1.24 m), and L is the total length of the reactor in the same direction (2.5 m). The mixing time, t_m, was determined by pulse–response experiments in batch mode (no, liquid flow through the reactor). It was determined as the time required to attain a 5% deviation from complete homogeneity after the injection of a tracer pulse was injected in the reactor. The mixing time, t_m, is a direct indicator of the mixing capacity of the reactor and allows the comparison with characteristic times of processes taking place inside the reactor.

2.3. Heat transfer measurements

Overall heat transfer coefficients were determined separately for the internal heat exchanger (heat transfer from the broth to the fluid circulating the heat exchanger) and for the outer surface exposed to air (heat exchange between the broth and the environment). The overall coefficient for the exchanger was determined filling the reactor with water and then circulating hot water (35 °C) through the heat exchanger and recording the temperature changes at the inlet and outlet of the heat exchanger and in the reactor. Since the environment was cooler than the reactor, heat was simultaneously lost to the surrounding air. Once the system reaches a steady state, the overall heat transfer coefficients for the internal and external sections of the reactor can be calculated from the following heat balances.

$$m_{water} \cdot Cp_{water} \cdot (T_{inlet} - T_{outlet}) = U_1 A_1 \frac{(T_{culture} - T_{inlet}) - (T_{culture} - T_{outlet})}{\ln(T_{culture} - T_{inlet})/(T_{culture} - T_{outlet})} \quad (10)$$

The left hand side of this equation represents the heat flow lost by the hot water circulating the heat exchanger, and the right hand side is the heat flow transferred to the water within the reactor. The overall heat transfer coefficient, U_1, can be calculated using Eq. (10), where m_{water} is the mass flow of hot water through the heat exchanger, T_{inlet} and T_{outlet} the temperatures at the inlet and outlet of the heat exchanger, $T_{culture}$ the temperature of the liquid inside the reactor, and A_1 is the external area of the heat exchanger.

The overall heat transfer coefficient, U_2, between the reactor and the surrounding air, can be calculated using Eq. (11), where T_{air} is the temperature of the air surrounding the reactor, and A_2 is the area of the reactor exposed to air.

$$m_{water} \cdot Cp_{water} \cdot (T_{inlet} - T_{outlet}) = U_2 A_2 (T_{culture} - T_{air}) \quad (11)$$

Experiments were done at different water flow rates, m_{water}, and aeration rates in order to study the influence of both variables on the overall heat transfer coefficients.

2.4. Solar radiation

The solar radiation was measured using a LICOR 200 sensor connected to a data acquisition board. Data were collected for three different surfaces: horizontal, vertical south-faced and vertical east-faced. For the horizontal surface only the upper face was considered whereas for the vertical surfaces the sensor was located on both sides to determine the overall irradiance intercepted by a photobioreactor positioned in the same way. Thus, the irradiance on the surfaces was measured each hour during the daylight period, which allowed the daily irradiance to be determined by integration of data. Measurements were performed on different dates, always on clear days, to determine the influence of the surface position on the overall irradiance intercepted.

In addition to experimental measurements, the solar radiation on a fixed surface can be estimated as a function of its location and position. Fig. 2 summarizes the main geometric considerations to take into account to estimate solar radiation on a given surface [25]. For a fixed location of latitude, ϕ, the extraterrestrial daily global radiation H_o, as a function of the day of the year n, declination δ, and sunrise solar angle ω_s, is given by the following equations:

$$H_o = \left(\frac{24}{\pi} I_{sc}\right)\left(1 + 0.033\cos\left(\frac{360n}{365}\right)\right) \times \left(\cos\phi\cos\delta\sin\omega_s + \frac{2\pi\omega_s}{360}\sin\phi\sin\delta\right) \quad (12)$$

$$\delta = 23.45\sin\left(360\frac{284+n}{365}\right) \quad (13)$$

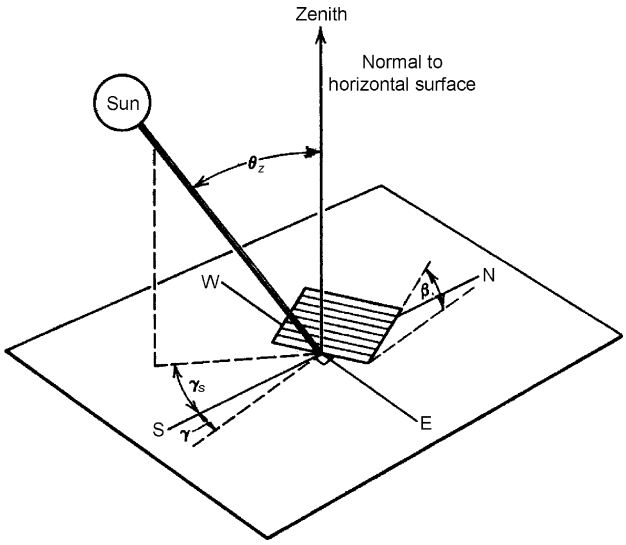

Fig. 2. Angles to be considered to determine the position of sun as a function of time, location and position of the surface.

$$\cos\omega_s = -\tan\delta\,\tan\phi \tag{14}$$

From the H_o value, the daily global radiation on a horizontal surface, H, can be calculated as a function of the transparency index of the atmosphere, Kh, which is available for long-term periods. For Almería, Spain (36°48′N; 2°54′W) the transparency index is 0.74 [26,27]. Using Kh is also possible to calculate the fraction of disperse to total global radiation to be calculated, H_d, and then the direct global radiation, H_b.

$$H = H_o\,\mathrm{Kh} \tag{15}$$

$$\frac{H_d}{H} = 1.39 - 4.03\,\mathrm{Kh} + 5.53\,\mathrm{Kh}^2 - 3.11\,\mathrm{Kh}^3 \tag{16}$$

$$H_b = H - H_d \tag{17}$$

For any given day, the hourly global radiation on a horizontal surface, G, can be calculated as a function of solar time, hs, which determines the solar angle, ω_s.

$$\omega_s = 15(12 - \mathrm{hs}) \tag{18}$$

$$G = H\left(\frac{\pi}{24}\right)(a + b\,\cos\omega)\left(\frac{\cos\omega - \cos\omega_s}{\sin\omega_s - (2\pi\omega_s/360)\,\cos\omega_s}\right) \tag{19}$$

$$a = 0.4090 + 0.5016\,\sin(\omega_s - 60) \tag{20}$$

$$b = 0.6609 - 0.4767\,\sin(\omega_s - 60) \tag{21}$$

Then, the hourly radiation on an tilted surface, β, oriented in a fixed position with respect to the south, γ, can be calculated. The direct, G_{rb}, and the diffuse, G_{rd}, components are first obtained separately and then the global hourly radiation on the tilted oriented surface, G_r, is calculated as the addition of both components. The calculations are detailed in the following equations:

$$R_b = \frac{\cos\theta}{\cos\theta_z} \tag{22}$$

$$R_d = \frac{1 + \cos\beta}{2} \tag{23}$$

$$\begin{aligned}\cos\theta = {} & (\sin\delta\,\sin\phi\,\cos\beta) - (\sin\delta\,\cos\phi\,\sin\beta\,\cos\gamma) \\ & +(\cos\delta\,\cos\phi\,\cos\beta\,\cos\omega) \\ & +(\cos\delta\,\cos\phi\,\sin\beta\,\cos\gamma\,\cos\omega) \\ & +(\cos\delta\,\sin\beta\,\sin\gamma\,\sin\omega)\end{aligned} \tag{24}$$

$$\cos\theta_z = (\sin\delta\,\sin\phi) + (\cos\delta\,\cos\phi\,\cos\omega) \tag{25}$$

$$G_{rb} = R_b G \tag{26}$$

$$G_{rd} = R_d G \tag{27}$$

$$G_r = G_{rb} + G_{rd} \tag{28}$$

Integration of the hourly global radiation, G_r, over a daytime period gives the daily global radiation on a surface tilted β and oriented γ to the south. Integration for the whole year gives the overall annual global radiation on the considered surface.

3. Results

3.1. Solar radiation

The methodology proposed in Eqs. (12)–(28) has been used to estimate the solar radiation on the flat photobioreactor surfaces (horizontal, vertical north/south and vertical east/west) as a function of position and location. As shown in Fig. 3A, the irradiance values obtained with the estimation are in good agreement with experimental determinations. Therefore, this methodology is proved useful for the estimation of the impinging irradiance and can be used for the correct design and operation of this type of photobioreactor. The results obtained for the studied location (Almería, Spain, 36°48′N; 2°54′W) show that the irradiance intercepted by a flat photobioreactor oriented east/west and a horizontal photobioreactor are quite similar. The daily global variations from winter (minimum) to summer (maximum) are also analogous. The annual variation of daily global radiation intercepted by a vertical photobioreactor oriented east/west is similar to that intercepted by a horizontal photobioreactor, with maximum and minimum values being reached in summer and winter, respectively. For horizontal photobioreactors the radiation intercepted ranged from 11 to 30 MJ/m^2 day, whereas for vertical photobioreactors oriented east/west the total radiation intercepted ranged from 13 to 29 MJ/m^2 day. On the other hand, the results obtained for the north/south oriented flat photobioreactor are quite different. In this case, the annual variation of daily global radiation was maximum in winter and minimum summer. The values obtained ranged from 26 to 16 MJ/m^2 day for winter and summer, respectively. For this location, vertical photobioreactors east/west oriented intercepted more radiation in winter

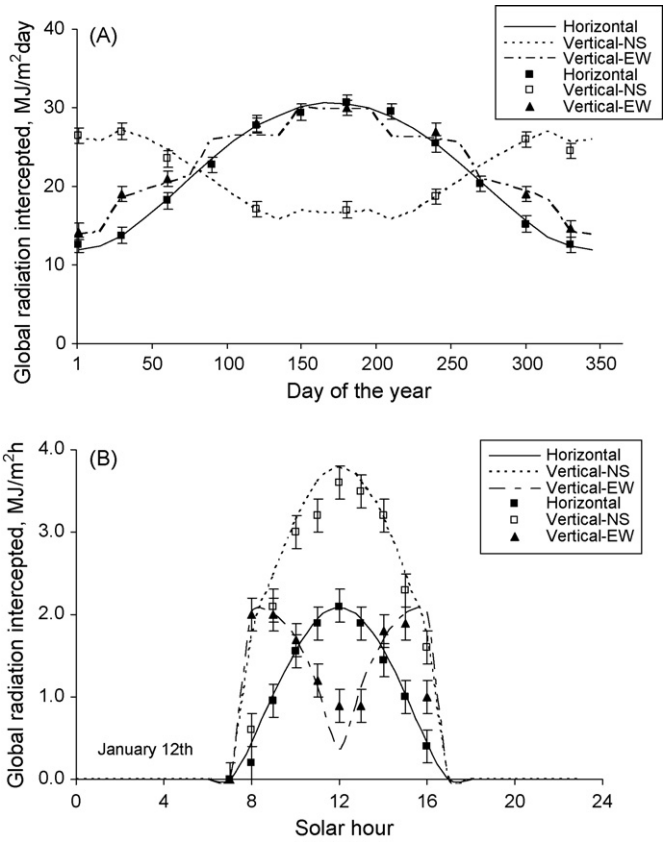

Fig. 3. Influence of position and orientation of photobioreactors in the capture of solar radiation over the year (A) and on a specific day (B), in Almería, Spain (36°48′N; 2°54′W). Lines correspond to simulated values using proposed Eqs. (12)–(28), whereas points correspond to experimental measurements.

than the horizontal surface (+17%), but is slightly less in summer (−3%). This means a homogenization of light availability over the year, in comparison with horizontal systems and an increase of 5% in total radiation intercepted. On the other hand, a vertical photobioreactors oriented north/south duplicates the solar radiation intercepted by a horizontal photobioreactor in winter, but obtains 65% less in summer. The overall annual radiation intercepted vertical north/south only increases 1% with respect to horizontal photobioreactors.

The hourly radiation intercepted is presented in Fig. 3B. The results show that the behaviour of the horizontal photobioreactor and the vertical north/south oriented photobioreactor are similar, whereas the vertical photobioreactor oriented east/west shows a totally different variation. For the latter the intercepted radiation is maximum during the first and last solar hours, because of the orientation towards sunrise and sunset of the main surfaces. At noon, the time of maximum solar radiation, there is a sharp decrease. Therefore, light availability during the daylight solar cycle is also more homogeneous for this configuration. For the location under study on a winter's day (January 12th), the daily global radiation intercepted by a east/west oriented vertical photobioreactor is 18% higher than that intercepted by a horizontal photobioreactor, while the global radiation intercepted by the north/south oriented vertical photobioreactor is double than the horizontal case.

3.2. Fluid-dynamics, mass transfer and mixing characterization

The fluid-dynamic characterization of the reactor comprised the influence of the air flow rate on the gas holdup and the volumetric mass transfer coefficient of the reactor (Fig. 4). Both parameters increased linearly with the air flow rate. Maximum values of 0.018 for holdup and 0.0063 1/s for the mass transfer coefficient were measured at the highest aeration rate tested 0.32 v/v/min, expressed as volume of air per culture volume and time (usual expression in microalgal biotechnology). This corresponded to a superficial gas velocity. The superficial gas velocity $U_G = 0.0076$ m/s (more usual in the engineering field). The superficial gas velocity U_G is easily derived from the air flow rate by multiplying this last one by the total volume of the culture, 0.25 m^3, and dividing by the cross-sectional area of the aerated zone, 0.175 m^2 (2.5 m × 0.07 m). The experiments were limited to low flow rates, under the usual 1 v/v/min utilized in low scale cultures, because the objective was to determine the optimal conditions for the operation of large-scale photobioreactors, and consequently the power consumption must be minimized.

The results of mixing are shown in Fig. 5. A variance of 0.24 was measured with no aeration with a sharp rise to 0.50 at the minimum air flow rate (0.003 v/v/min). Increasing aeration rates up to 0.091 v/v/min increased the mixing intensity to a maximum variance of 0.84. Above this value the mixing induced by the aeration diminished slightly with increasing aeration rates till values of variance of 0.71. The variance due to the aeration was very significant in the system for every flow rate, the behaviour being that of a mixed-tank system. The dispersion coefficient changed in a similar fashion, ranging from 0.012 to 0.024 m^2/s. However, the mixing time varied in the opposite way, being lower than 200 s in all experiments of aeration flow rate, and even at the extremely low rate of 0.003 v/v/min (Fig. 5). The mixing time decreased with aeration flow rate down to values of 100 s at 0.091 v/v/min. Above this aeration rate the mixing time increased up to values of 130 s at 0.311 v/v/min, indicating a reduction in the mixing.

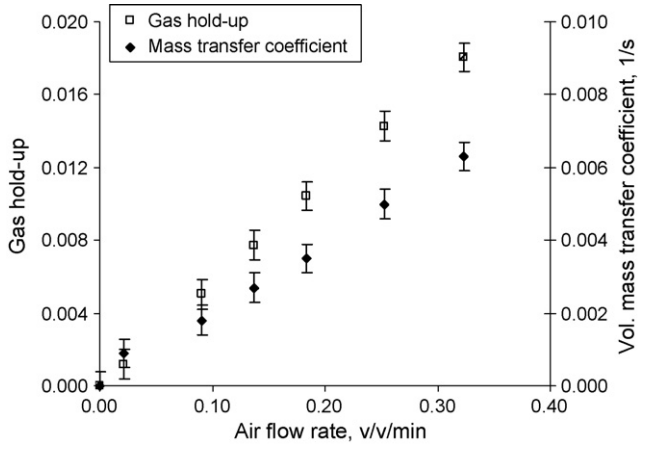

Fig. 4. Influence of the aeration rate in the gas holdup and volumetric mass transfer coefficient of the flat plate photobioreactor used.

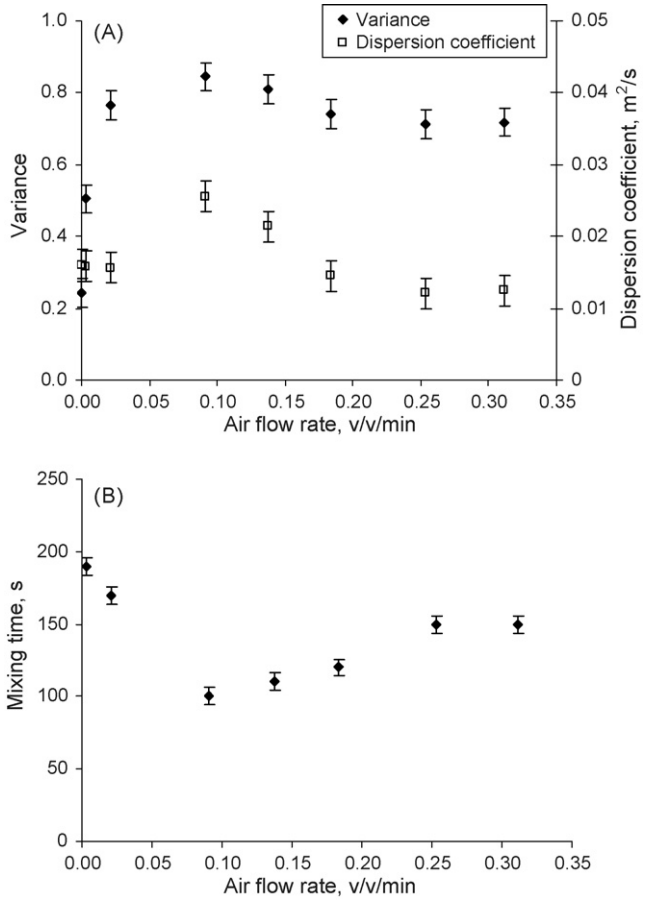

Fig. 5. Influence of the aeration rate on the variance and dispersion coefficient (A), and mixing time (B) in the flat plate photobioreactor used. Variance was calculated from pulse–response experiments data using Eq. (7). From this value, the dispersion coefficient was calculated using Eq. (9). Mixing time was determined as the time required since the addition of a tracer to attain 5% deviation from complete homogeneity.

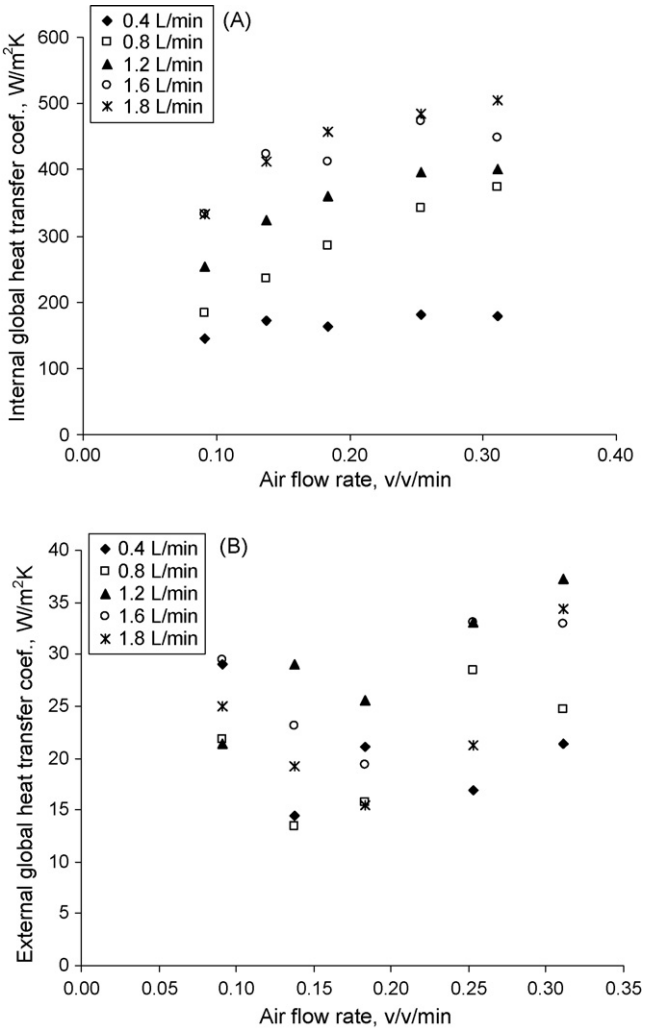

Fig. 6. Influence of the aeration rate and liquid velocity through the internal exchanger in the internal (A) and external (B) heat transfer coefficients of the flat plate photobioreactor used.

3.3. Heat transfer measurements

Culture temperature is an important parameter to be controlled in outdoor photobioreactors. Water-spray systems are often used to avoid overheating. However, the cooling capacity of spray systems is limited and its application is only possible under certain environmental conditions (temperature, humidity, etc.). The use of heat exchangers for the temperature control of photobioreactors requires the study of the overall heat transfer coefficients between the culture and the fluid circulating within the internal heat exchanger, as well as between the culture broth photobioreactor and the surrounding air. These parameters were determined in the flat panel photobioreactor, considering the influence of air flow rate and water flow through the internal heat exchanger (Fig. 6). The results show that the overall heat transfer coefficient for the internal heat exchanger was much higher than the overall heat transfer coefficient between the culture and the environment surrounding the photobioreactor, with maximum values of 505 and 37 W/m^2 K, respectively. The internal heat transfer coefficient was mainly a function of the water flow through the heat exchanger, although enhancement of the air flow rate also improved the internal heat transfer coefficient. As regards the external heat transfer coefficient, these results do not show a defined variation, with values ranging from 13 to 37 W/m^2 K. It is important to note that experiments were performed indoors under controlled conditions; the value of the external heat transfer coefficient may be higher under outdoor conditions due to wind and atmospheric perturbations.

4. Discussion

4.1. Solar radiation

The productivity of any microalgal system is a direct function of the total solar radiation intercepted. This, for a specific placement, depends on the orientation and type of photobioreactor employed. By analogy with solar panels, photobioreactors should automatically tilt to the zenith angle of sun to maximize the amount of solar radiation intercepted [28]. In this way productivity can be enhanced by 35% with respect to vertical photobioreactors [21]. However, the scalability of such systems can prove difficult. If a fixed tilt is used it must be as close as

possible to the latitude at which the photobioreactor is located [21,29]. In these conditions, productivity can be increased by 17% with respect to vertical photobioreactors [21]. However, the higher cost of this design compared to-tilt designs does not compensate for the productivity enhancement. For this reason, only horizontal and vertical photobioreactors have been widely used for mass production of microalgae. In both cases orientation is usually south-facing [29,30]. However, the solar radiation intercepted may vary significantly with orientation. For horizontal systems this is not an important consideration, but it is a major issue for vertical systems. For the location under study, the vertical photobioreactors east/west orientation maximizes the solar radiation intercepted over the year (Fig. 3A). With this orientation the photobioreactors intercept 5% more radiation than horizontal systems on an annual basis, and what is more important: the radiation intercepted in winter, when the cultures are more photo-limited, is increased while in summer the proportion of intercepted radiation decreases, which is good in this time of the year when the cultures tend to be more photo-inhibited [27]. However, this increase is a function of the location of the reactor (Fig. 7). For latitudes above 35°N the east-faced/west-faced orientation are favourable to north/south, the higher the latitude the higher the increase in the solar radiation intercepted. On the contrary, for latitudes under 35°N the north/south orientated reactors intercept more radiation and the difference is more pronounced the closer to the equator.

The position of the reactor also influenced the type of radiation intercepted. In horizontal photobioreactors direct radiation is the most important contribution [26,27], while in the vertical photobioreactors the proportion of disperse radiation is dominant [21,29]. Disperse radiation has been reported to be more efficient for microalgal cultures. Indeed, the photosynthetic efficiency of vertical photobioreactors has been reported to be higher than optimal tilt reactors, reaching values of 20% [21]. This is due to the fact that low irradiance levels normally result in higher photosynthetic efficiencies, this is, when cells are growing under irradiance levels far from saturating. This can be accomplished by increasing the light-receiving surface of the photobioreactor per land square meter, a technique usually referred to as "dilution" of light.

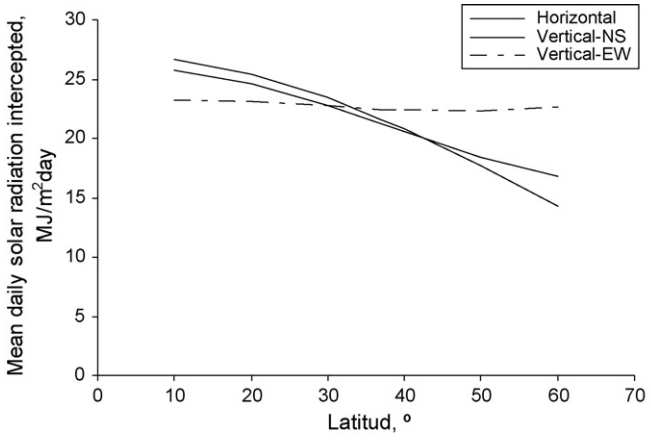

Fig. 7. Influence of latitude and position of the photobioreactor in the annual mean daily solar radiation intercepted. Values obtained using proposed Eqs. (12)–(28).

Regarding the specific design of the closed photobioreactor, three different kinds have been proposed: tubular, flat panel and column reactors. Only flat panel and tubular photobioreactors have been built to sizes exceeding 1000 L [30,31,49], whereas for column systems a maximum of 125 L has been proposed as optimum [29,42]. In the case of tubular photobioreactors, different designs of the same concept have been proposed. Among these, are worth to mention horizontal loops [7,8,49], helical loops [32,33], and vertical loops [2]. In view of these proposals it is obvious that the arrangement of the tubes is a main issue to be addressed first. Torzillo et al. [34] proposed a two plane tubular photobioreactor that improves the yield of the system. This design was later optimized to capture 87% of total radiation but duplicating the total volume of culture per land surface unit, thus enhancing the yield of the system [14]. The analysis of solar radiation performed in this paper suggests that the use of vertically arranged walls of horizontal tubes east-faced/west-faced is the best option to install tubular photobioreactors. An alternative would be to use vertical flat panel photobioreactors with the same orientation.

4.2. Fluid-dynamic, mass transfer and mixing characterization

The major advantage of flat panel reactors is that they have a much shorter oxygen path than tubular reactors, in which oxygen accumulation may become damaging. However, tubular photobioreactor are well known and can be designed to overcome this limitation by improving the fluid-dynamic and mass transfer capacity and can be built even at sizes exceeding 1000 L [31,49]. Therefore, for a fair comparison a characterization of the fluid-dynamics in flat plate photobioreactor was performed in this work. The analysis carried out confirms that the power supply is the major variable influencing the behaviour of the system. The gas holdup increased with the specific power input in accordance with previously published data (Fig. 8). The holdup data followed a potential relationship with the power supply analogous to that previously referenced (Eq. (29)) [23].

$$\varepsilon = 3.32 \times 10^{-4} \left(\frac{P_G}{V_L} \right)^{0.97} \quad (29)$$

However, the measured values of gas holdup were slightly higher than the predicted by Eq. (29). This may be due to a recirculation of gas bubbles that took place because the gas flow within the reactor was not totally uniform. Although the bottom of the reactor was completely flat, lack of complete uniformity in the placement of the sparger leaded to zones with less hydrostatic pressure near the edges of the panel which caused slightly higher more air bubbled in these zones. This caused a circular movement of the liquid and gas bubbles which contributed to retain part of the gas stream by dragging down part of the bubbles, thus enhancing the gas holdup. The power supply also influences the mass transfer capacity of the reactor (Fig. 8). The volumetric gas–liquid mass transfer coefficient has been referenced to

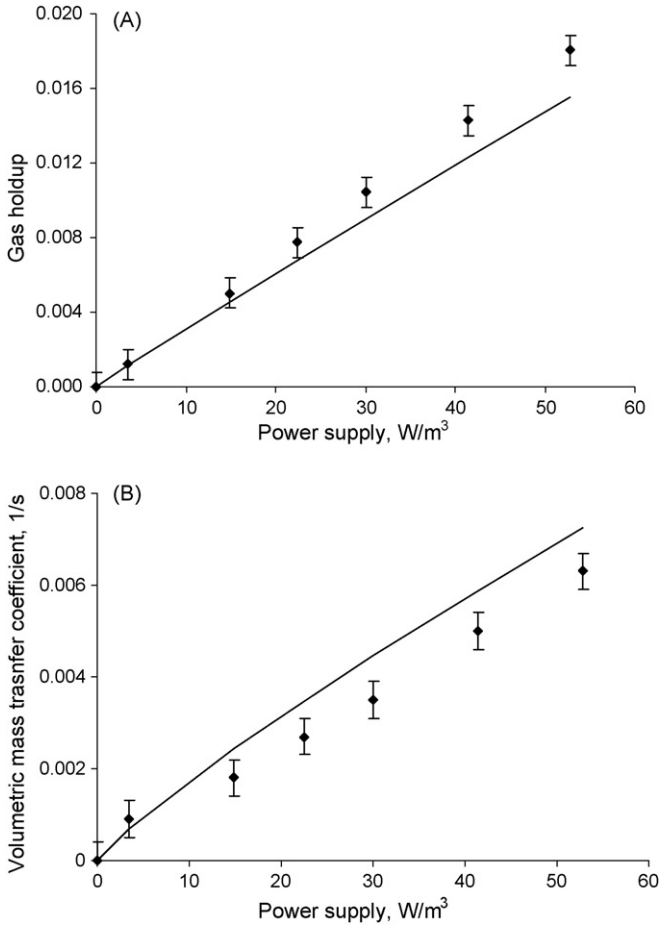

Fig. 8. Influence of power supply in the gas holdup (A) and volumetric mass transfer coefficient (B) of the flat plate photobioreactor used. Lines correspond to values simulates using referenced Eq. (29) and (30) whereas points correspond to experimental measurements.

increase potentially with the power supply (Eq. (30)) [23].

$$K_L a_L = 2.39 \times 10^{-4} \left(\frac{P_G}{V_L} \right)^{0.86} \quad (30)$$

Our results agree with this behaviour, although Eq. (30) slightly overestimates the mass transfer coefficient. Nonetheless, it is important to note that, in spite of the low power supply used, the volumetric mass transfer coefficient reached values of 0.0063 1/s. This result is important because over-accumulation of dissolved oxygen has harmful effects on the cells. Oxygen concentrations above air saturation generally inhibit photosynthesis in microalgae [35]. In cultures of *Anabaena azollae* carried out in vertical alveolar panels the yield of the cultures decreased when the dissolved oxygen accumulated to 400%Sat. [12]. In *P. tricornutum* the photosynthetic activity clearly decreased at dissolved oxygen concentrations exceeding 100%Sat., and to some extent even also below this value. The maximum photosynthesis rate of 0.0036 mol O_2/m^3 s measured at 100%Sat. was reduced by a 15% at dissolved oxygen concentrations of 0 and 300%Sat. At dissolved oxygen concentrations of 475%Sat., the photosynthesis rate fell sharply to 0.0016 mol O_2/m^3 s (55% reduction) [7].

For every photobioreactor design considered, it is possible to ensure a sufficient mass transfer capacity so that photosynthetically generated oxygen does not over-accumulate. Considering a maximum biomass productivity of 2.0 g/L day with 50% carbon content in the biomass and a photosynthesis ratio of 1 mol O_2/molCO_2, a mass transfer coefficient of 0.006 1/s would suffice to prevent dissolved oxygen concentration to go over 300%Sat. This mass transfer capacity in the flat panel photobioreactor can be attained with 53 W/m^3 power supply (Fig. 8). To attain the same mass transfer capacity 40 W/m^3 are requested in bubble columns [42,48], and 2400–3200 W/m^3 in tubular photobioreactors [14,15,36]. Zhang et al. [37] reported a biomass productivity of 1.0 g/L day, with *Synechocystis aquatilis* in outdoor flat panels, at aeration rates of 0.05 v/v/min, corresponding to a power supply of 10 W/m^3. This shows that oxygen removal in the exhaust gas-phase is substantially easier in flat panel and bubble column reactors than in tubular ones, although it is also possible to design tubular photobioreactors to avoid excessive oxygen accumulation.

The low power supply required for the flat panel photobioreactor, with a maximum of 53 W/m^3, is an important advantage because of the sensitivity of many microalgal cells to damage caused by intense turbulence [38–41]. Cell damage has been reported when the turbulence intensity gives rise to fluid microeddies of size similar to cell dimensions [41]. In bubble columns, the maximum power supply that *Dunaliella tertiolecta* can bear was 98 W/m^3 [39], whereas the maximum power supply tolerable for *P. tricornutum* ranged from 230 W/m^3 [48] to 270 W/m^3 [40]. The highest power supply in aerated systems ranged from 280 W/m^3 in flat plate photobioreactors [6,21] to 200 W/m^3 in bubble columns or internal airlift systems employing split cylinders and draught tube sparger photobioreactors [42]. However, the power supply in tubular photobioreactors is usually much higher. In helical photobioreactors the power supply ranged from 800 to 3400 W/m^3 [15,33], similar to 2500 W/m^3 in horizontal tubular photobioreactors [36]. In spite of the higher power supply in tubular photobioreactors damage to algal cells has never been documented in this type of photobioreactors [42]. This can be due to the culture velocity in tubular loops usually not exceeding 0.5 m/s, which is less than half the threshold damage value of 1.14 m/s [14]. These data highlight the different nature of stress in bubble column-flat plate photobioreactors and tubular photobioreactor.

In addition to gas holdup and mass transfer capacity, the power supply also determines the mixing inside the reactor. Fig. 9 shows that the dispersion coefficient increases hyperbolically with the power supply from the initial value of 0.015 m^2/s when no aeration is supplied, to 0.026 m^2/s at power supply of 14.8 W/m^3. Above this value the dispersion coefficient decreases, remaining at values of 0.012 m^2/s at power supplies up to 40 W/m^3. Only at very low power supplies the behaviour of the system agrees with that referenced for bubble columns, i.e. the dispersion coefficient increases potentially with the superficial gas velocity or power supply (Eq. (31), [43]; Eq. (32), [44]), whereas the mixing time decreases (Eq. (33), [45]). At higher

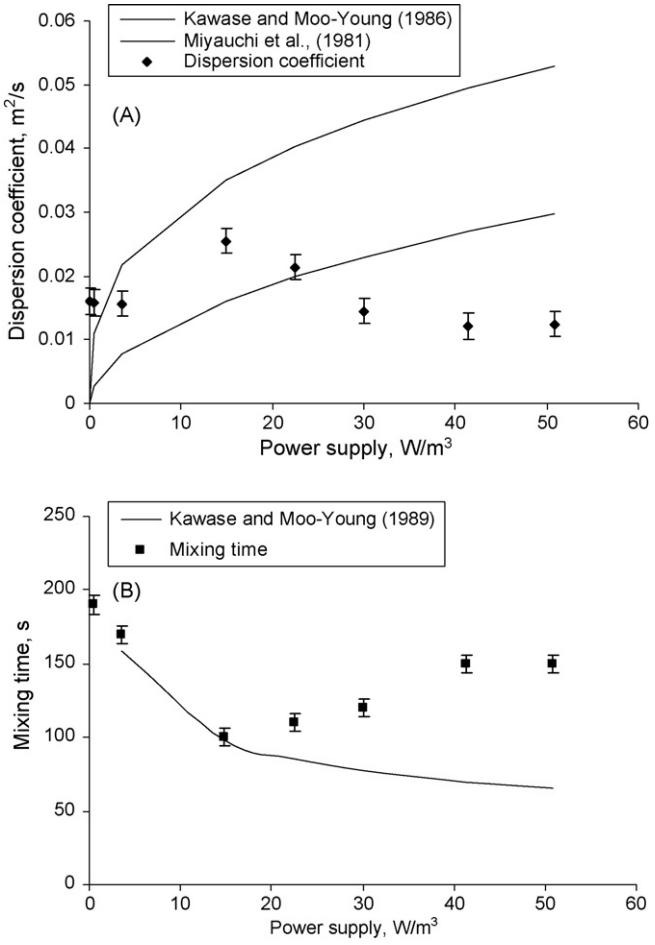

Fig. 9. Influence of power supply in the dispersion coefficient (A) and mixing time (B) of the flat panel photobioreactor used. Line corresponds to values simulated using referenced Eqs. (33)–(35), whereas points correspond to experimental data.

power supplies the behaviour is mixed but close to plug-flow, the dispersion coefficient scarcely increases with the power supply and the mixing time even increases [14,15].

$$D_z = 0.5 g^{1/4} U_G^{1/2} d^{5/4} \quad (31)$$

$$D_z = 0.343 g^{1/3} U_G^{1/3} d^{4/3} \quad (32)$$

$$t_m = 0.343 g^{1/3} U_G^{1/3} d^{4/3} \quad (33)$$

Results shows that in bubble columns and internal airlift photobioreactors the mixing is higher than in flat panel photobioreactors, with dispersion coefficients of 0.03–0.04 m^2/s being measured at power supplies lower than 200 W/m^3 [29,46]. On the other hand, tubular reactors have higher power supplies and the behaviour is closer to plug-flow. To achieve a dispersion coefficient of 0.04 m^2/s in a 0.06 m tubular photobioreactors it is necessary to supply up to 2400 W/m^3 [14], whereas in a 0.03 m helical photobioreactor operated at power supply of 3200 W/m^3 the dispersion coefficient was 0.012 m^2/s [15]. In the latter, the mixing time ranged from 20 h under normal operation conditions to more than 100 h at extremely low air flow rate, as opposed to 100–150 s to achieve complete mixing in the flat panel photobioreactor, or 60 s in bubble columns [46]. Moreover, in tubular photobioreactors the dispersion coefficient was virtually constant regardless the liquid flow rate in the tube or the aeration rate in the riser [14]. It is important to note that whatever the design the power supply favoured the mixing in the reactor. However, the particular power supply value and the best fit model to represent the fluid-dynamics influence in the different reactors is a function of the design. In tubular photobioreactors the loop is not aerated, and therefore there is a poor axial mixing in this section, being limited to the small volume of the reactor that is aerated. As a result, axial nutrient concentration gradients may develop, especially if the reactor is not fed continuously with fresh medium. This problem is important when operating in semicontinuous mode, as happen in the referred helical reactor where mixing time is of the same order of magnitude as the time interval between the dilution periods (24–48 h) [14,15]. In flat panel photobioreactors an optimum aeration rate of 0.05 v/v/min has been proposed sufficient to improve the mixing and mass transfer without introducing damage by stress [37].

4.3. Heat transfer measurements

The power supply also determines the heat transfer capacity of the photobioreactor. The overall resistance to heat transfer of the internal heat exchanger can be considered as the addition of three individual resistances: inner convection (water circulating through the inner space of the heat exchange tube to its inner surface), tube wall conduction and external convection (tube external surface to water outside the heat exchanger). Each of these contributions can be calculated separately. The Dittus–Boelter equation was used to determine the individual heat transfer coefficient inside the tube (the inverse of individual resistance). The contribution of the tube wall was calculated by physical considerations taking into account geometry and thermal conductivity of the stainless steel, the tube material. Since the overall heat transfer coefficient was obtained through experimentation, the only remaining individual coefficient, the external resistance between the tube and the aerated water could be straightforwardly calculated. The results obtained show that the conductivity of stainless steel represents only 4% of the overall heat transfer resistance, whereas the convection of water circulating inside the heat exchanger represents a 60%. This can be attributed to the low water flow rate used. The values of the individual heat transfer coefficient for this side ranged from 300 to 1000 W/m^2 K. In spite of the low aeration rate only 36% of the overall heat transfer resistance corresponded to the external side. The external individual heat transfer coefficient increased with aeration rate from 400 to 2000 W/m^2 K as shown in Fig. 10. This behaviour agrees with what has been previously reported for bubble columns (Eq. (34), [47]; Eq. (35), [44]), although the experimental data obtained in the present work are lower than what could be expected for these systems. Using the experimental data, an empirical correlation was obtained for the overall heat transfer coefficient, referred to the external tube side, with Reynolds number (Eq. (36)). However, more experiments are necessary to determine the variation of heat transfer coefficients

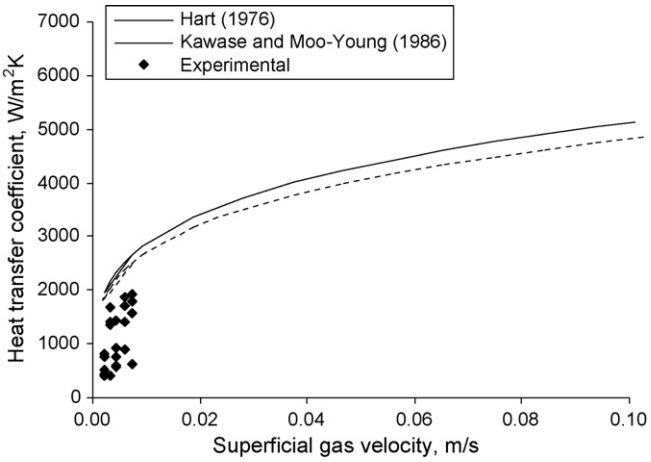

Fig. 10. Influence of superficial gas velocity in the individual heat transfer coefficient for the side of bubbled water of flat panel photobioreactor. Line corresponds to values simulated using referenced Eqs. (34) and (35), whereas points correspond to experimental data.

in flat panel reactors with design and operational variables.

$$\frac{h}{\rho_L Cp U_g}\left(\frac{Cp\mu_L}{k_L}\right)^{0.6} = 0.125\left(\frac{U_g^3\rho_L}{\mu_L g}\right)^{-0.25} \quad (34)$$

$$\frac{h\mathrm{Dc}}{k} = 0.134\, Re^{3/4} Pr^{1/3} Fr^{-1/4} \quad (35)$$

$$h = 4.32\, Re^{0.71} \quad (36)$$

The result show that the internal heat exchanger used is superior to water-spray systems, giving a global heat transfer coefficient of up to 500 W/m^2 K. Moreover, the use of heat exchangers would enable the use of heat accumulation systems to greatly improve the energetic yield of the system. Heat accumulation systems circulate water from a reservoir of appropriate dimensions. This water heats up during the central hours of the daylight period as heat is withdrawn from the reactor to avoid overheating. During the night period the heated water can be circulated through the heat exchanger to warm up the culture as the reservoir water cools. Operating in this way, it has been possible to reduce the daily temperature differences in outdoor tubular photobioreactors from 12 to 5 °C, reducing the power consumption to one-third compared to the energy that would be consumed to operate the system without the heat accumulator (data not shown). For the correct design of this type of system it is mandatory to know the solar radiation intercepted by the photobioreactor, as well as the heat transfer coefficients of the reactor, both internal and external, all of which are analyzed in this paper.

5. Conclusions

It can be concluded that one of the major aspects determining the productivity of a microalgal system is the location, deployment and orientation of the reactor. The vertical deployment facing east/west is favourable, as it increases the culture volume per surface unit without greatly reducing the total radiation intercepted. Moreover this orientation reduces direct beam radiation on the reactor surface while increasing disperse radiation, which is more favourable. Regarding the type of photobioreactor, both tubular and flat panel photobioreactors have already been scaled up to volumes of over 1000 L. However, flat panel photobioreactors require less power supply than tubular photobioreactors to achieve enough mass transfer, mixing and heat transfer capacity. On the other hand, stress by aeration has been sometimes reported in flat panel photobioreactors whereas it has never been reported in tubular photobioreactors. In both cases, knowledge of the heat transfer capacity of the reactor allows the correct design of heat accumulation systems, thus greatly enhancing the energetic efficiency of the system. The characterization presented allows the correct design and operation of this type of photobioreactor for the production of microalgae.

Acknowledgements

This research was supported by the Ministerio de Ciencia y Tecnología (CTQ 2004-07628-C02-01/PPQ), Junta de Andalucía (P05-CVI-422), Plan Andaluz de Investigación III (CVI 173, CVI 263), and ENDESA GENERACIÓN S.A.

References

[1] M.A. Borowitzka, Commercial production of microalgae: ponds, tanks, tubes and fermenters, J. Biotechnol. 70 (1) (1999) 313–321.
[2] O. Pulz, Photobioreactors: production systems for phototrophic microorganisms, J. Appl. Microbiol. Biotechnol. 57 (3) (2001) 287–293.
[3] A. Richmond, Z. Cheng-Wu, Optimization of a flat plate glass reactor for mass production of *Nannochloropsis* sp. outdoor, J. Biotechnol. 85 (2001) 259–269.
[4] J.C. Goldman, Outdoor algal mass cultures. II. Photosynthetic yield limitations, Water Res. 13 (1979) 119–136.
[5] A. Richmond, Large scale microalgal culture and applications, in: F.E. Round, D.J. chapman (Eds.), Progress in Phycological Research, vol. 7, Biopress Ltd., Bristol, 1990.
[6] Q. Hu, Y. Zarmi, A. Richmond, Combined effects of light intensity, light-path and culture density on output rate of *Spirulina platensis* (Cyanobacteria), Eur. J. Phycol. 33 (1998) 165–171.
[7] E. Molina, J. Fernández, F.G. Acién, Y. Chisti, Tubular photobioreactors design for algal cultures, J. Biotechnol. 92 (2001) 113–131.
[8] C. Gudin, D. Chaumont, Solar biotechnology study and development of tubular solar receptors for controlled production of photosynthetic cellular biomass, in: W. Palz, D. Pirrwitz (Eds.), Proceedings of the Workshop E.C., Contractor's Meeting, Capri, Reidel, Dordrecht, 1983, pp. 184–193.
[9] E. Molina, F. García, J.A. Sánchez, J.A. Urda, F.G. Acién, J.M. Fernández, Outdoor chemostat culture of *Phaeodactylum tricornutum* UTEX 640 in a tubular photobioreactor for the production of eicosapentaenoic acid, Biotechnol. Appl. Biochem. 20 (1994) 279–290.
[10] Y. Watanabe, D.O. Hall, Photosynthetic production of the filamentous cyanobacterium *Spirulina platensis* in a cone-shaped helical tubular photobioreactor, Appl. Microbiol. Biotechnol. 44 (1996) 693–698.
[11] J. Doucha, K. Livansky, Novel outdoor thin-layer high density microalgal culture system: productivity and operational parameters, Algol. Stud. 76 (1995) 129–147.
[12] M.R. Tredici, P. Carlozzi, G. Chini, R. Materassi, A vertical alveolar panel for outdoor mass cultivation of microalgae and cyanobacteria, Biores. Technol. 38 (1991) 153–159.
[13] R. Samon, A. Leduy, Multistage continuous cultivation of blue-green alga *Spirulina maxima* in the flat tank photobioreactors with recycle, Can. J. Chem. Eng. 63 (1985) 105–112.

[14] F.G. Acién, J.M. Fernández, J.A. Sánchez, E. Molina, Y. Chisti, Airlift-driven external loop tubular photobioreactors for outdoor production of microalgae: assessment of design and performance, Chem. Eng. Sci. 56 (2001) 2721–2732.
[15] D.O. Hall, F.G. Acién, E. Cañizares, K. Rao, E. Molina, Outdoor helical tubular photobioreactors for microalgal production: modelling of fluid-dynamics and mass transfer and assessment of biomass productivity, Biotechnol. Bioeng. 82 (1) (2003) 62–73.
[16] J.S. Burlew, in: J.S. burlew (Ed.), Algal Culture from Laboratory to Pilot Plant, Carnegie Institution of Washington, Washington, D.C., 1953, pp. 235–281.
[17] M.R. Tredici, R. Materassi, From open ponds to vertical alveolar panels: the Italian experience in the development of reactor for the mass cultivation of photoautotrophic micro organisms, J. Appl. Phycol. 4 (1992) 221–231.
[18] O. Pulz, N. Gerbsch, R. Bacholz, Light energy supply in plate-type and light diffusing optical fiber bioreactors, J. Appl. Phycol. 7 (1995) 145–149.
[19] Q. Hu, A. Richmond, Productivity and photosynthetic efficiency of *Spirulina platensis* as affected by light intensity, algal density and rate of mixing in a flat plate photobioreactor, J. Appl. Phycol. 18 (1996) 139–145.
[20] Q. Hu, H. Gutterman, A. Richmond, A flat inclined modular photobioreactor for outdoor mass cultivation of photoautotrophs, Biotechnol. Bioeng. 51 (1996) 51–60.
[21] Q. Hu, D. Fairman, A. Richmond, Optimal tilt angles of enclosed reactors for growing photoautotrophic microorganisms outdoors, J. Ferment. Bioeng. 85 (1998) 230–236.
[22] M.R. Tredici, L. Rodolfi, Reactor for industrial culture of photosynthetic microorganisms. World Patent WO 2004/074423 A2 (to Università degli Studi di Firenze, Italia), 2004.
[23] Y. Chisti, Airlift Bioreactors, Elsevier, London, 1989.
[24] O. Levenspiel, The Chemical Reactor Omnibook, Bu OSU Book Stores Inc., Corvallis, OR, 1979, p. 97330.
[25] R.Y.H. Liu, R.C. Jordan, The interrelationship and characteristic distribution of direct, diffuse and total solar radiation, Solar Energy 7 (1960) 53–65.
[26] F.G. Acién, F.G. García, J.A. Sánchez, J.M. Fernández, E. Molina, A model for light distribution and average solar irradiance inside outdoor tubular photobioreactors for the microalgal mass culture, Biotechnol. Bioeng. 55 (1997) 701–714.
[27] F.G. Acién, F.G. García, J.A. Sánchez, J.M. Fernández, E. Molina, Modelling of biomass productivity in tubular photobioreactors for microalgal cultures: effects of dilution rate, tube diameter and solar irradiance, Biotechnol. Bioeng. 58 (1998) 605–616.
[28] J.A. Duffie, W.A. Beckman, Solar Engineering of Thermal Processes, John Wiley & Sons, Inc., New York, 1980.
[29] F. García, A. Contreras, F.G. Acién, J.M. Fernández, E. Molina, Use of concentric-tube airlift photobioreactors for microalgal outdoor mass cultures, Enzyme Microb. Technol. 24 (1999) 164–172.
[30] Z. Cheng-Wu, O. Zmora, R. Kopel, A. Richmond, An industrial-size flat plate glass reactor for mass production of *Nannochloropsis* sp. (Eustigmatophyceae), Aquaculture 195 (2001) 35–49.
[31] E. Molina, J.M. Fernandez, F.G. Acien, J.F. Sanchez, J. Garcia, J.J. Magan, J. Perez, Production of lutein from the microalga Scenedesmus almeriensis on a industrial size photobioreactor: case study, in: Proceedings of the 6th European Workshop Biotechnology of Microalgae, Potsdam, Germany, 2005.
[32] L.F. Robinson, A.W. Morrison, M.R. Bamforth, 1987, European Patent 0,239,272, March 6, 1987 (Biotechna Ltd.).
[33] Y. Watanabe, J. de la Noüe, D.O. Hall, Photosynthetic performance of a helical tubular photobioreactor incorporating the cyanobacterium *Spirulina plantensis*, Biotechnol. Bioeng. 47 (1995) 261–269.
[34] G. Torzillo, P. Carlozzi, B. Pushparaj, E. Montaini, R. Materassi, A two plane tubular phoptobioreactor for outdoor culture of *Spirulina*, Biotechnol. Bioeng. 42 (1993) 891–898.
[35] S. Aiba, Growth kinetics of photosynthetic microorganisms, Adv. Biochem. Eng. 23 (1982) 85–156.
[36] F. Camacho, F.G. Acién, J.A. Sánchez, F. García, E. Molina, Prediction of dissolved oxygen and carbon dioxide concentration profiles in tubular photobioreactors for microalgal culture, Biotechnol. Bioeng. 62 (1) (1999) 71–86.
[37] K. Zhang, S. Miyachi, N. Kurano, Photosynthetic performance of a cyanobacterium in a vertical flat-plate photobioreactor for outdoor microalgal production and fixation of CO_2, Biotechnol. Lett. 23 (2001) 21–26.
[38] H.J. Silva, T. Cortiñas, R.J. Ertola, Effect of hydrodynamic stress on *Dunaliella* growth, J. Chem. Technol. Biotechnol. 40 (1987) 41–49.
[39] T. Suzuki, T. Matsuo, K. Ohtaguchi, K. Koide, Gas-sparged bioreactors for CO_2 fixation by *Dunaliella tertiolecta*, J. Chem. Technol. Biotechnol. 62 (1995) 351–358.
[40] A. Contreras, F. García, E. Molina, J.C. Merchuk, Interaction between CO_2-mass transfer, light availability and hydrodynamic stress in the growth of *Phaeodactylum tricornutum* in a concentric tube airlift photobioreactor, Biotechnol. Bioeng. 60 (1998) 318–325.
[41] Y. Chisti, Shear sensitivity, in: M.C. Flickinger, S.W. Drew (Eds.), Encyclopedia of Bioprocess Technology, Wiley, New York, 1999, pp. 2379–2406.
[42] A. Sánchez, A. Contreras, F. García, E. Molina, Y. Chisti, Comparative evaluation of compact photobioreactors for large scale monoculture of microalgae, J. Biotechnol. 70 (1999) 249–270.
[43] T. Miyauchi, S. Furusaki, S. Morooka, Y. Ikeda, Transport phenomena and reaction in fluidized catalyst beds, Adv. Chem. Eng. 11 (1981) 275–448.
[44] Y. Kawase, M. Moo-Young, Influence of non-Newtonian flow behaviour on mass transfer in bubble columns with and without draft tubes, Chem. Eng. Commun. 40 (1986) 67–83.
[45] Y. Kawase, M. Moo-Young, Mixing time in bioreactors, J. Chem. Tech. Biotechnol. 44 (1989) 63–75.
[46] F. Camacho, A. Sánchez, M.C. Cerón, F. García, E. Molina, Y. Chisti, Mixing in bubble columns: a new approach for characterizing dispersion coefficients, Chem. Eng. Sci. 59 (2004) 4369–4376.
[47] W.F. Hart, Heat transfer in bubble-agitated systems: a general correlation, Ind. Eng. Chem. Res. 15 (1976) 109–114.
[48] C. Brindley, M.C. García-Malea, F.G. Acién, J.M. Fernández, J.L. García, E. Molina, Influence of power supply in the feasibility of *Phaeodactylum tricornutum* cultures, Biotechnol. Bioeng. 87 (6) (2002) 723–733.
[49] M.R. Tredici, G. Chini, Scale-up of photobioreactors to commercial size, in: P. Kretschmer, al. et (Eds.), Proceedings of the 2nd European Workshop on Biotechnology of Microalgae, 1995, pp. 21–24.